



Journal of Applied and Computational Mechanics



Research Paper

Influence of Pressure on the Frequency Spectrum of Micro and Nanoresonators on Hinged Supports

Marat A. ILGAMOV^{1,2} , Akim G. KHAKIMOV¹ 

¹ Mavlyutov Institute of Mechanics, Ufa, 450054, Russia, Email: ilgamov@anrb.ru

² Blagonravov Institute of Mechanical Engineering, Moscow, 101990, Russia, Email: hakimov@anrb.ru

Received October 20 2020; Revised January 25 2021; Accepted for publication January 26 2021.

Corresponding author: A.G. KHAKIMOV (hakimov@anrb.ru)

© 2021 Published by Shahid Chamran University of Ahvaz

Abstract. Eigenfrequencies of bending oscillations are determined for a resonator with rectangular cross-sections mounted on hinged supports. Consideration is given to the surface effect caused by the interaction between gas pressure and the difference in the areas of the resonator's convex and concave surfaces. Changes in the frequency spectrum are examined at the presence of both concentrated and uniformly distributed masses attached to the resonator's surface. The solution of the inverse problem enables the identification of attached masses using changes of eigenfrequencies.

Keywords: Resonator, Surface effect, Bending oscillations, Eigenfrequencies, Direct and inverse problems.

1. Introduction

Among multiple applications of micro and nanofilms, nanowires and nanotubes, one should also mention their use as detectors and sensors in chemistry, biology, etc. [1-3]. Because of the unique application, much attention in literature is paid to studying their performance properties. For example, [4, 5] give an overview of four hundred papers mainly devoted to cantilever resonators made of nanofilms and nanowires.

Due to a small thickness of films, wires and tubes, virus particles, DNA molecules, etc. adsorbed on their surface lead to a distinct change in the resonator's frequency spectrum. In this case intermolecular interactions, depending on the number of molecules on the surface, are theoretically taken into account [5].

The smaller is the resonator, the higher is its sensitivity (quality factor). Since the crosswise dimensions are much less than the longitudinal one, the primary movement of the device is the bending deformation of 1D elastic beam with different cross-section shapes. The resonators can have a laminated structure depending on their purpose. For example, outer piezo layers make it possible not only to maintain oscillations, but also to generate weak electric current when exciting bending oscillations with another source [6]. In [7], it is reported on self-suspended DNA nanobundles as ultrasensitive nanomechanical resonators for structural studies of DNA-ligand complexes. Electrostatically actuated resonators have demonstrated great potential in a wide range of applications, such as sensors, communication devices, logic gates, and quantum measurements [8]. To detect and identify different bioparticles and estimate their dimensions, a mechanical nanosensor is introduced in [9]. The governing equation of motion is derived from the Hamilton's principle. The Galerkin approximation is applied to discretize the nonlinear equation. In [10], the dynamic instability of a cantilever nanobeam connected to a horizontal spring is analyzed.

Since the resonators in question are characteristic of a large surface-area-to-volume ratio, the surface effects play a noticeable role in their dynamics. As a rule, these effects manifest themselves in inverse proportions to the film thickness and wire diameter. When describing their dynamics, account was taken for surface tension, difference in elastic properties of the subsurface layer and the main volume of the material, thermo-elastic dissipation, contact-medium effects, etc. [1-14]. However, in the theory of resonators there is still no account for the interaction between the curvature of the mid-surface of the film and axial line of the wire, on the one hand, and average pressure in the surfaces, on the other hand. Similar account was made in [15, 17] for the static and dynamic problems on wire and film curvatures. In this case consideration was also given in [16, 17] to the aforesaid difference in the elastic properties. Longitudinal oscillations of nanorods with attached point mass are studied in [18]. Eigenfrequencies of a nanorod with concentrated mass were obtained for different boundary conditions. Bending oscillations of a uniform nanobeam with one attached mass (direct problem) and identification of attached mass (inverse problem) are investigated in [19]. The nanobeam is described using the modified theory of deformation energy. In [20], the initial coordinate, the magnitude of the distributed mass attached to a step-shaped rod and also the area ratio are determined using three lower eigenfrequencies of longitudinal oscillations.

As shown in [21, 22], the applicability of classical equations of deformation of thin elements like rods and plates to describe their behavior can be assessed according to such integral characteristics as eigenfrequencies. The first two eigenfrequencies of bending oscillations of the rod with clamped ends and dimensions $b = 4.08$ nm, $h = 4.08$ nm, $L = 49$ nm, modulus of elasticity $E = 0.39 \cdot 10^5$ MPa and density of the material $\rho = 19300$ kg/m³ determined via MD simulation (molecular dynamics) are equal to $f_1 =$



2.71 — 2.78, $f_2 = 7.28 — 7.33$ GHz. According to the ratios in continuum mechanics based on the Kirchhoff hypotheses, the same frequencies are equal to 2.83 and 7.81 GHz, respectively. The inclusion of the lateral shear and rotational inertia of the cross section (Timoshenko model) leads to even closer results (2.78 and 7.43 GHz [21]). Large deviations in the results for higher harmonics are explained by the reduction of the ratio between half-wavelength and thickness, when the model of a thin body gives higher error values. In view of these considerations we shall resort to the ratios used in classical mechanics [23, 24].

In this work, we evaluate the frequency spectrum of a resonator on hinged supports taking into account the interaction between the average excess pressure on the resonator's surface and the curvature of the axial line as well as the effect of axial loading. Using the inverse problem solution, we determine some parameters of the resonator and also the magnitudes and coordinates of the attached mass.

2. Problem Statement

An elastic strip with thickness h , width b and length L is fixed to hinged supports (Figure 1a). It is assumed that the smallest size h has order 10 nm, and the ratio L/h has order $10^1 — 10^3$, therewith $h < b$. The self-weight of the strip is ignored.

Linear bending oscillations of the strip are described by equation [23]

$$EJ \frac{\partial^4 w}{\partial x^4} - P \frac{\partial^2 w}{\partial x^2} + \rho b h \frac{\partial^2 w}{\partial t^2} = q, \quad J = \frac{bh^3}{12(1-\nu^2)}, \tag{1}$$

where E, ν, ρ are the modulus of elasticity, the Poisson's ratio and the density of the material, x, t are the longitudinal coordinate and the time, w is the deflection, P is the longitudinal stretching force, q is the transverse distributed force.

Beginning with the synthesis research papers [23, 24] and up to the current literature, it is assumed that the lateral force q distributed through pressures $p_0 + p_1$ and $p_0 + p_2$ between the strip's upper and lower surfaces is equal to $q = p_2 - p_1$. The assembly pressure p_0 , including the atmospheric one, is all-around and also affects the strip's edge zones. It is assumed that there are no strains in this case. The excess pressures p_1, p_2 affect only the strip's surfaces. The lengths dx_1, dx_2 of the upper and lower surfaces along the x axis under cylindrical bending are equal [23] (Figure 1b)

$$dx_{1,2} = \left(1 + \varepsilon_x \left(\pm \frac{h}{2}\right)\right) dx, \quad \varepsilon_x \left(\pm \frac{h}{2}\right) = -\left(\pm \frac{h}{2} \frac{\partial^2 w}{\partial x^2}\right), \tag{2}$$

where ε_x is the longitudinal strain. The expression for $\varepsilon_x(w)$ follows from the Kirchhoff hypotheses on a slight change in thickness and normal section curve under bending of a thin body [23]. In this case, pressures acting on the lateral surfaces ($y = 0, b$) are put in equilibrium. As it follows from the equality $q dx = (p_2 dx_2 - p_1 dx_1) b$ and expressions (2) [16, 17],

$$q = (p_2 - p_1) b + p_m b h \frac{\partial^2 w}{\partial x^2}, \quad p_m = \frac{p_1 + p_2}{2}. \tag{3}$$

Account for the attached mass of the external medium and radiation entering it gives $p_1 \neq p_2$. These factors will be ignored that can be justified with light gases. In the case of medium movement relative to the resonator the former may exert a distinct influence [25]. Let us assume that the velocity head of the external medium is considerably less than the average pressure p_m , and this movement is not taken into account. Thus, let us examine the case when $p_1 = p_2 = p$. Then, the expression for q from (3) can be represented as

$$q = p b h \frac{\partial^2 w}{\partial x^2}. \tag{4}$$

The longitudinal force P in equation (1) will be determined for a strip in the case of fixed edges $x = 0, L$. This force is governed by the excess pressure p and can be defined using Hooke's law for the case of the strain $\varepsilon_x = 0$,

$$\sigma_x = \frac{E}{1-\nu^2} (\nu \varepsilon_y + \nu \varepsilon_z), \sigma_y = -\frac{E}{1-\nu^2} (\varepsilon_y + \nu \varepsilon_z), \sigma_z = \frac{E}{1-\nu^2} (\varepsilon_z + \nu \varepsilon_y). \tag{5}$$

Since $\sigma_y = -p, \sigma_z = -p$, it follows from (5) that $\varepsilon_y = \varepsilon_z = -(1-\nu)p/E$. Thus, the axial compression force arises under the action of strip's confinement with pressure p

$$P = \sigma_x b h = -\frac{2 p b h \nu}{1 + \nu}. \tag{6}$$

Accepting the function of bending flexure in the form of $w(x) \exp(i\omega t)$ and using hereinafter the notations $\xi = x/L, w = w/L$, equation (1) with account for (4), (6) and the conditions of the hinged attachment are presented in the form

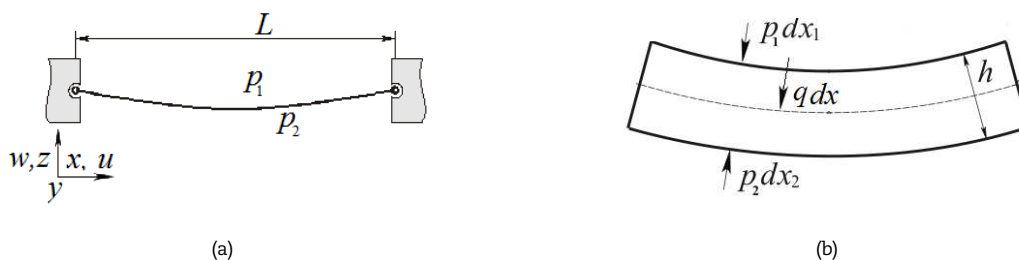


Fig. 1. (a) Example for clamping the resonator: the pressure effect on the edge areas does not create a longitudinal force in the unit. (b) The element dx of the mid-surface of the curved resonator.



$$\frac{\partial^4 w}{\partial \xi^4} - 2\alpha \frac{\partial^2 w}{\partial \xi^2} - k^2 w = 0, \quad \alpha = \frac{pbhL^2(1-\nu)}{2EJ(1+\nu)}, \quad k^2 = \frac{\rho bhL^4 \omega^2}{EJ}, \quad (7)$$

$$w = 0, \quad \partial^2 w / \partial \xi^2 = 0 \quad (\xi = 0; 1), \quad (8)$$

where ω is the circular frequency. This equation holds good for the case of no longitudinal displacements in both supports of the strip. If one of the supports allows a free longitudinal displacement, but there is no excess pressure at its end, it will be necessary to exclude the value ν from the expression for α . For the freely sliding support in the case of the action of pressure on the end face $\alpha = 0$, since $P = -pbh$.

3. Influence of Pressure on the Frequency Spectrum

The solution of equation (7) has the form

$$w(\xi) = A \cos(\lambda_1 \xi) + B \sin(\lambda_1 \xi) + C \operatorname{ch}(\lambda_2 \xi) + D \operatorname{sh}(\lambda_2 \xi),$$

$$\lambda_1^2 = -\alpha + \sqrt{\alpha^2 + k^2}, \quad \lambda_2^2 = \alpha + \sqrt{\alpha^2 + k^2}.$$

Boundary conditions (8) at $\xi = 0$ give $A = C = 0$. As it follows from the conditions at $\xi = 1$,

$$\begin{aligned} B \sin \lambda_1 + D \operatorname{sh} \lambda_2 &= 0, \\ B \lambda_1^2 \sin \lambda_1 - D \lambda_2^2 \operatorname{sh} \lambda_2 &= 0. \end{aligned} \quad (9)$$

The corresponding determinant is written as

$$(\lambda_1^2 + \lambda_2^2) \sin \lambda_1 \operatorname{sh} \lambda_2 = 0.$$

Since $\lambda_1^2 + \lambda_2^2 \neq 0$, $\operatorname{sh} \lambda_2 \neq 0$ at $\lambda_2 > 0$, then $\sin \lambda_1 = 0$, from which it follows that $\lambda_1 = n\pi$ ($n = 1, 2, \dots$). Thus, the frequency parameter k from (7) is equal to

$$k_n^2 = n^2 \pi^2 (n^2 \pi^2 + 2\alpha). \quad (10)$$

It follows from the first equation (9) that $D = 0$. Natural modes have the form $B_n \sin n\pi\xi$. As seen from (10), an increase in eigenfrequencies takes place with the positive value of the excess pressure p ($\alpha > 0$), and vacuuming ($p < 0$, $\alpha < 0$) is accompanied by their decrease compared to the case $p = 0$. For higher harmonics the influence of the external pressure is reduced. With account for (7), (10) the formula can be written for the frequency spectrum as

$$f_n = \frac{\omega_n}{2\pi} = \frac{n^2 \pi c h}{2L^2} \sqrt{1 + \frac{2\alpha}{n^2 \pi^2}}, \quad c = \sqrt{\frac{E}{12(1-\nu^2)\rho}}. \quad (11)$$

At $E = 76 \cdot 10^3$ MPa, $\nu = 0.25$, $\rho = 10500$ kg/m³, $h = 20$ nm, $L = 500$ nm, $p = 1$ MPa, the parameter is $2\alpha/\pi^2 = 0.0054$. Thus, in this case there is no distinct influence of the external pressure on the resonator's frequency spectrum. If with the same data $p = 5$ MPa, $L = 2000$ nm, then $2\alpha/\pi^2 = 0.43$. In this case the first two frequencies are equal to $f_1 = 7.865$, $f_2 = 27.654$ MHz. Without account for the parameter α , they are equal to $f_1 = 6.565$, $f_2 = 26.262$ MHz.

In the case of the resonator's assembly under high pressures, for example, $p_0 = 5$ MPa, and drop to the atmospheric pressure (0.1 MPa), the excess pressure is equal to $p = -4.9$ MPa. Then, with the same data $2\alpha/\pi^2 = -0.50$. The frequencies are equal to $f_1 = 4.973$, $f_2 = 24.824$ MHz.

Figure 2a gives the dependence at $n = 1$ according to formula (11). It is seen that as the external pressure increases the eigenfrequencies of oscillations increase as well.

Using the first frequency of bending oscillations, we can determine, by means of formula (11), the excess gas pressure for the case of no longitudinal displacements in both supports with their edges isolated from the external medium

$$p = \frac{\rho}{1-\nu} \left(4L^2 f_1^2 - \frac{\pi^2 c^2 h^2}{L^2} \right),$$

for example, for the frequency 7.25 MHz the pressure p is equal to 2.521 MPa.

Let us consider the case of high pressure and large ratio of the resonator's length to its thickness. If in the example under consideration, we take $h = 15$ nm, $L = 5000$ nm, $p = 50$ MPa, then $2\alpha/\pi^2 \approx 77$ with one freely sliding end and the first harmonic. Then only the second member can be preserved in (11) under the radical. In this case,

$$f_1 = \frac{1}{2L} \sqrt{\frac{p}{\rho}} = 6.9 \text{ MHz}.$$

Thus, in this limiting case the first eigenfrequency does not depend on the modulus of elasticity and thickness. This is explained by the fact that because of the small ratio h/L the bending stiffness proportional to h^3 is low, and the first member in equation (7) is small compared to the second member proportional to h . In accordance with the conventional theory of resonators (without account for the surface effect, $\alpha = 0$) $f_1 \approx 0.78$ MHz.

4. Frequency Spectrum at Uniformly Distributed Attached Mass

Let the uniformly distributed mass m_s of some substance be adsorbed on the resonator's surface. It is assumed that this attached mass does not change the resonator's bending stiffness. Then the parameter k^2 will be written in the form



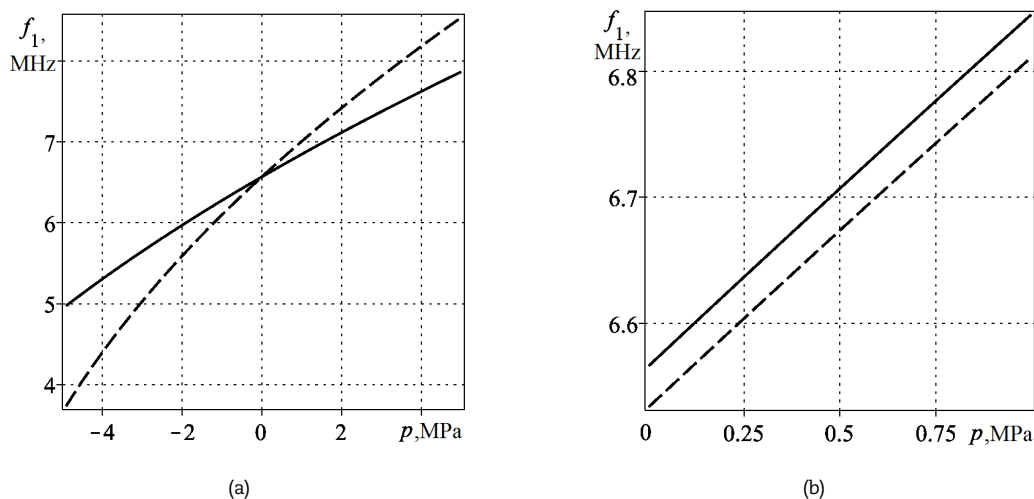


Fig. 2. (a) Dependence of the first eigenfrequency f_1 on the excess pressure p . The solid line is for the case of no longitudinal displacements in both supports of the rod. The dashed line is for the sliding support. (b) dependence of the first eigenfrequency on the excess pressure p for the parameter $\beta = 0.01, 0$ (dashed and solid lines, respectively).

$$k^2 = \frac{\rho b h L^4 \omega^2 (1 + \beta)}{EJ}, \quad \beta = \frac{m_s}{\rho h}. \tag{12}$$

With account for (11), (12), the formula of the frequency range can be written as

$$f_n = \frac{n^2 \pi c h}{2L^2} \sqrt{\frac{1}{1 + \beta} \left(1 + \frac{2\alpha}{n^2 \pi^2} \right)}.$$

Figure 2b shows the dependence of the first eigenfrequency on the pressure p at different values of the parameter β . It is seen that as the uniformly distributed attached mass increases and the average pressure the eigenfrequencies of oscillations decrease as well.

5. Frequency Spectrum in the Case of Attached Point Mass

Consideration is given to the resonator’s bending oscillations with the point mass m attached at the point $x = x_c$. Indicating the functions by indices 1, 2 in the regions $0 \leq x \leq x_c, x_c \leq x \leq L$, we write the conditions for junction solutions at $x = x_c$ (equality displacement, rotation angles, moments, shearing forces)

$$w_1 = w_2, \quad \frac{\partial w_1}{\partial \xi} = \frac{\partial w_2}{\partial \xi}, \quad \frac{\partial^2 w_1}{\partial \xi^2} = \frac{\partial^2 w_2}{\partial \xi^2}, \quad \frac{\partial^3 w_1}{\partial \xi^3} - \frac{\partial^3 w_2}{\partial \xi^3} = m^* k^2 w_1, \quad (\xi = \xi_c), \quad m^* = \frac{m}{\rho FL}.$$

Satisfying these conditions and boundary conditions (8) of the solution, we obtain

$$\sin \lambda_1 + m^* \eta = 0, \quad \eta = k^2 \left\{ \lambda_2 \cos \lambda_1 \operatorname{sh} \lambda_2 \sin^2(\lambda_1 \xi_c) - \lambda_1 \sin \lambda_1 \operatorname{ch} \lambda_2 \operatorname{sh}^2(\lambda_1 \xi_c) + \right. \\ \left. + \sin \lambda_1 \operatorname{sh} \lambda_2 [\lambda_1 \operatorname{sh}(\lambda_2 \xi_c) \operatorname{ch}(\lambda_2 \xi_c) - \lambda_2 \sin(\lambda_1 \xi_c) \cos(\lambda_1 \xi_c)] \right\} / (\lambda_1 \lambda_2 (\lambda_1^2 + \lambda_2^2) \operatorname{sh} \lambda_2). \tag{13}$$

Since $\lambda_1^2 + \lambda_2^2 \neq 0, \operatorname{sh} \lambda_2 \neq 0$ at $\lambda_2 > 0$, it follows from (13) that

$$\sin \lambda_1 = -m^* \eta, \quad \lambda_1 = n\pi - \arcsin(-m^* \eta) = n\pi + \arcsin(m^* \eta), \quad (n = 1, 2, \dots)$$

Thus, the frequency parameter k from (7) is equal to

$$k_n = \left(n\pi + (-1)^{n+1} \arcsin(m^* \eta) \right)^2 \sqrt{1 + \frac{2\alpha}{\left(n\pi + (-1)^{n+1} \arcsin(m^* \eta) \right)^2}}. \tag{14}$$

As it follows from (7), (14),

$$f_n = \frac{ch \left(n\pi + (-1)^{n+1} \arcsin(m^* \eta) \right)^2}{2\pi L^2} \sqrt{1 + \frac{2\alpha}{\left(n\pi + (-1)^{n+1} \arcsin(m^* \eta) \right)^2}}.$$

Calculations are performed for the following parameters of the system [21]: $E = 0.39 \cdot 10^5$ MPa, $b = 4.08$ nm, $h = 4.08$ nm, $L = 49$ nm, $\rho = 19,300$ kg/m³. To determine the frequencies we apply the method of successive approximations. The dependence of the first eigenfrequency of oscillations on the number of molecules with the mass 33 kDa ($1 \text{ kDa} = 1.66 \cdot 10^{-24}$ kg) preset for the coordinate $\xi_c = 0.5$ at different excess pressure values is shown in Figure 3a. It is seen that as the number of molecules n_1 increases and the excess pressure decreases the frequency of oscillations decreases as well.



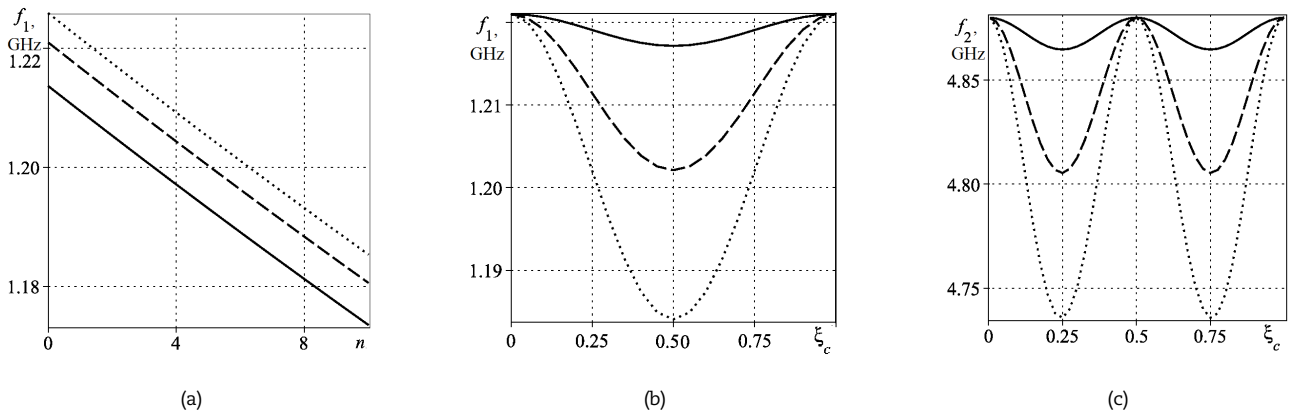


Fig. 3. (a) Dependence of the first eigenfrequency of oscillations on the number of molecules with the mass 33 kDa at different values of the excess pressure $p = -4.9, 1.0, 5.0$ MPa (solid, dashed and dotted lines, respectively). Dependence of the first (b) and second (c) eigenfrequencies of oscillations on the coordinate ξ_c of the attached mass $m = 300, 150, 30$ kDa (dotted, dashed and solid lines, respectively).

The dependence of the first eigenfrequency of oscillations on the coordinate ξ_c for the average pressure $p = 1$ MPa at different values of the attached mass is given in Figure 3b.

When the point mass is placed at the resonator’s center, the eigenfrequency of oscillations decreases. The dependence of the second eigenfrequency of oscillations on the coordinate ξ_c for the pressure $p = 1$ MPa at different values of the attached mass is given in Figure 3c. The second eigenfrequency of the resonator does not depend on the point mass placed at the center. This is explained by coincidence of the mass with the knot of oscillations.

6. Finding the Value and Coordinate of the Attached Point Mass using Two Frequencies of Bending Oscillations

Since the dependence of the first and the second frequencies of bending oscillations on the coordinate ξ_c is periodical, the solution of the inverse problem on finding the coordinate and value of the attached point mass should be $O_i(\xi_i, M_i) \ i = 1, 2, \dots, n_2$ for the selected regions, where n_2 is the number of regions, $\Xi_i \leftrightarrow ((\xi_c)_{\min} \dots (\xi_c)_{\max})$, $M_i \leftrightarrow (m^{\min} \dots m^{\max})$. The number of regions depends on the first and second preset frequencies and regions $O_i(\xi_i, M_i)$. For example, for the frequencies $f_1 = 1.20$ and $f_2 = 4.80$ GHz there are two regions to determine the coordinate ξ_c and the value of the attached point mass m . The second region is symmetrical relative to the first one with its axis of symmetry in the resonator’s center. The solution to the set of two equations for the first and the second frequencies gives the value of the coordinate $\xi_c = 0.334$ and the attached point mass $m = 221.7$ kDa in the first region. Thus, using two frequencies of bending oscillations we can determine the coordinate and attached point mass adsorbed on the resonator’s surface.

7. Comparison of the Influence of Surface Effects

The distributed force (4) can be treated as the surface effect manifestation. Let us compare its influence on frequencies with that of the known surface effects governed by the difference of elastic properties in the thin surface layer and the strip’s main volume. According to [9, 11, 13], the effective bending and expansion stiffnesses of the strip are determined by the formulae

$$(EJ)_s = EJ + \frac{1}{2}E_s b h^2 + \frac{1}{6}E_s h^3, \quad (Ebh)_s = Ebh + 2\tau_s(b + h), \tag{15}$$

where E is the elastic modulus in beam of dimension MPa, E_s is the surface elastic modulus of dimension MPa·m, τ_s is the residual surface stress of dimension MPa·m. It is assumed that some thickness and the Poisson’s ratio enter implicitly to E_s and τ_s . It should be noted that in [9] the last member of the last expression (15) is equal to $2\tau_s b$. Instead of (7), we have the equation

$$(1 + \eta) \frac{\partial^4 w}{\partial \xi^4} - 2(\mu + \alpha) \frac{\partial^2 w}{\partial \xi^2} - k^2 w = 0, \quad \eta = \frac{E_s h^2}{2EJ} \left(b + \frac{h}{3} \right), \quad \mu = \frac{\tau_s L^2 (b + h)}{EJ}. \tag{16}$$

On repeating the solution to equation (16) like above, we shall obtain the values of circular frequencies

$$\omega_n = \omega_n^0 \sqrt{1 + \eta + \frac{2(\mu + \alpha)}{n^2 \pi^2}}, \quad \omega_n^0 = \left(\frac{n\pi}{L} \right)^2 \sqrt{\frac{EJ}{\rho h}}, \tag{17}$$

where ω_n^0 are the frequencies determined without account for surface effects. As it follows from (17), the parameters μ and α do not have any influence of higher harmonics.

Relationships

$$\frac{\alpha}{\mu} = \frac{pbh}{2\tau_s(b + h)}, \quad \frac{2\alpha}{n^2 \pi^2 \eta} = \frac{2pbL^2}{n^2 \pi^2 E_s h(b + h/3)}$$

vary within wide limits.

The paper [9] presents the following data: $L = 90$ nm, $b = 18$ nm, $h = 3.5$ nm, $E = 1.76 \cdot 10^5$ MPa, $\nu = 0.33$, $E_s = 10^{-4}$ MPa·m, $\tau_s = 10^{-7}$ MPa·m. If we assume that $p = 1$ MPa, free longitudinal sliding along one of the supports, $n = 1$, then $\alpha/\mu = 0.017$, $2\alpha/(\pi^2 \eta) = 0.0046$. Here, the expression for $(Ebh)_s$ is taken as in [9]. In this case $2\alpha/\pi^2 = 0.0038$. Thus, with these data the pressure parameter α does not have any influence on the frequency. It is small compared to the parameters μ and η . At $L = 3500$ nm, $h = 35$ nm, $p = 5$



MPa, these relationships are equal to $\alpha/\mu=0.875$, $2\alpha/(\pi^2\eta)=3.29$, and the absolute value of the parameter is $2\alpha/\pi^2 = 0.284$. Since

$$\eta \approx \frac{6E_s}{Eh}, \quad \mu \approx \frac{12\tau_s L^2}{Eh^3}, \quad \alpha \approx \frac{5pL^2}{Eh^2},$$

further increase in the thickness h at the invariable relationship of L/h results in less influence of the parameters μ and η at the invariable relationship of α . Since this paper deals with the analysis of the influence exerted by the excess pressure p on the frequencies of oscillations, we confine ourselves only to an account for the parameter α .

8. Conclusion

Large specific surface areas of micro and nanoresonators is are responsible for a distinct manifestation of different surface effects. The bending model of an elastic strip pivoted at its ends suggests the simplest way to determine the excess pressure influence of the external medium on its oscillations. This remained unaccounted up to now. This influence on the frequency range is determined by the nondimensional parameter α using formula (7). It is proportional to the ratio of the pressure and the elastic modulus of the material, and also the squared ratio of the resonator's length and its thickness (or its diameter in the case of a circular cross-section).

As the excess pressure of the external medium increases, the frequencies of oscillations increase as well. Under the negative excess pressure (vacuuming) the frequencies tend to decrease. For actual input parameters these changes are of essential significance, especially for lower harmonics. At high pressures of the external medium and large ratio between the resonator's length and thickness the frequency range slightly depends on the modulus of elasticity and thickness. Only the length and the ratio between the pressure and density of the material play a decisive role. These results cannot be obtained in the context of the conventional theory of resonators. In view of a large difference in the results, it seems reasonable to conduct a corresponding experimental study.

Using the first frequency of bending oscillations it becomes possible to determine the external environment pressure. As the uniformly distributed attached mass increases and the excess pressure decreases, the eigenfrequencies of oscillations decrease as well. As the attached mass (number of molecules) at the resonator's center increases, odd frequencies of bending oscillations tend to decrease. Even eigenfrequencies of the resonator's bending oscillations do not depend on the point mass placed at the center. Using two frequencies of bending oscillations we can determine the attached point mass and its coordinate using the resonator's length. A comparison is given for the influence of excess pressure on the resonator's first frequency and surface effects known from literature. With realistic values of the parameters, these effects can be of the same order.

Author Contributions

The manuscript was written through the contribution of all authors. All authors discussed the results, reviewed, and approved the final version of the manuscript.

Conflict of Interest

The authors declared that there are no potential conflicts of interest with respect to the research, authorship, and publication of this article.

Funding

The work was supported by the state budget for the state task (No. 0246-2019-0088).

Nomenclature

b	Width [m]	J	Moment of inertia [m ⁴]
h	Thickness [m]	x	Longitudinal coordinate [m]
L	Length [m]	dx ₁ , dx ₂	Lengths [m]
t	Time [s]	w	Bending flexure [m]
E _s	Surface elastic modulus [MPa·m]	P	Longitudinal stretching force [N]
τ _s	Residual surface stress [MPa·m]	E	Modulus of elasticity [MPa]
ρ	Density of the material [kg/m ³]	ν	Poisson's ratio
p ₀	Assembly pressure [MPa]	q	Transverse distributed force [N/m]
m	Attached mass [kg, Da]	p ₁ , p ₂	Excess pressures [MPa]
k	Frequency parameter	p _m	Average pressure [MPa]
A, B, C, D	Constants	f ₁ , f ₂	Frequencies [Hz]
A _i , B _i , C _i , D _i	Constants, i=1,2	λ ₁ , λ ₂	Wave number
ω	Circular frequency [rad/s]	m _s	Distributed mass [kg]
n	Number of frequency	ε _x , ε _y , ε _z	Strains
α, μ, η	Parameters	σ _x , σ _y , σ _z	Normal stress [MPa]

References

- [1] O'Connell, A.D., Hofheinz, M., Ansmann, M., Bialczak, R.C., Lenander, M., Lucero, E., Neeley, M., Sank, D., Wang, H., Weides, M., Wenner, J., Martinis, J.M., Cleland, A.N., Quantum ground state and single-phonon control of a mechanical resonator, *Nature*, 464, 2010, 697–703, DOI: 10.1038/nature08967.
- [2] Burg, T.P., Godin, M., Knudsen, S.M., Shen, W., Carlson, G., Foster, J.S., Babcock, K., Manalis, S.R., Weighing of biomolecules, single cells and single nanoparticles in fluid, *Nature*, 446, 2007, 1066–1069, DOI: 10.1038/nature05741.
- [3] Husale, S., Persson, H.H.J., Sahin, O., DNA nanomechanics allows direct digital detection of complementary DNA and microRNA targets, *Nature*, 462, 2009, 1075–1078, DOI: 10.1038/nature08626.
- [4] Raman, A., Melcher, J., Tung, R., Cantilever dynamics in atomic force microscopy, *Nano Today*, 3(1–2), 2008, 20–27, DOI: 10.1016/S1748-0132(08)70012-4.



- [5] Eom, K., Park, H. S., Yoon, D. S., Kwon, T., Nanomechanical resonators and their applications in biological/chemical detection: Nanomechanics principles, *Physics Reports-Review Section of Physics Letters*, 503 (4–5), 2011, 115–163, DOI: 10.1016/j.physrep.2011.03.002.
- [6] Elnathan, R., Kwiat, M., Patolsky, F., Voelcker, N. H., Engineering vertically aligned semiconductor nanowire arrays for applications in the life sciences, *Nano Today*, 9(2), 2014, 172–196, DOI: 10.1016/j.nantod.2014.04.001.
- [7] Stassi, S., Marini, M., Allione, M., Lopatin, S., Marson, D., Laurini, E., Pricl, S., Pirri, C. F., Ricciardi, C., Fabrizio, E. D., Nanomechanical DNA resonators for sensing and structural analysis of DNA-ligand complexes, *Nature Communications*, 10, 2019, 1–10, DOI: 10.1038/s41467-019-09612-0.
- [8] Jaber, N., Hafiz, M. A. A., Kazmi, S. N. R., Hasan, M. H., Alsaleem, F., Ilyas, S., Younis, M. I., Efficient excitation of micro/nano resonators and their higher order modes, *Scientific Reports*, 9(319), 2019, DOI:10.1038/s41598-018-36482-1.
- [9] SoltanRezaee, M., Bodaghi, M., Simulation of an electrically actuated cantilever as a novel biosensor, *Scientific Reports*, 10(3385), 2020, DOI: 10.1038/s41598-020-60296-9.
- [10] Tavakolian, F., Farrokhhabadi, A., SoltanRezaee, M., Rahmanian, S., Dynamic pull-in of thermal cantilever nanoswitches subjected to dispersion and axial forces using nonlocal elasticity theory, *Microsystem Technologies*, 25(3), 2019, 19–30, DOI: 10.1007/s00542-018-3926-y.
- [11] He, J., Lilley, C. M., Surface stress effect on bending resonance of nanowires with different boundary conditions, *Applied Physics Letters*, 93, 2008, 263108, DOI: 10.1063/1.3050108.
- [12] He, J., Lilley, C. M., Surface effect on the elastic behavior of static bending nanowires, *Nano Letters*, 8, 2008, 1798–1802, DOI: 10.1021/nl0733233.
- [13] Wu, J. X., Li, X. F., Tang, A. Y., Lee, K. Y., Free and forced transverse vibration of nanowires with surface effects, *Journal of Vibration and Control*, 23, 2017, 2064–2077, DOI: 10.1177/1077546315610302.
- [14] Wang, F., Abedini, A., Alghamdi, T., Onsorynezhad, S., Bimodal approach of a frequency-up-conversion piezoelectric energy harvester, *International Journal of Structural Stability and Dynamics*, 4, 2019, DOI:10.1142/S0219455419500901.
- [15] Ilgamov, M. A., Flexural vibrations of a plate under changes in the mean pressure on its surfaces, *Acoustical Physics*, 64(5), 2018, 605–611, DOI: 10.1134/S1063771018050032.
- [16] Ilgamov, M. A., Influence of surface effects on bending and buckling of nanowires, *Doklady Physics*, 64(9), 2019, 345–348, DOI: 10.1134/S1028335819090040.
- [17] Ilgamov, M. A., The influence of surface effects on bending and vibrations of nanofilms, *Physics of the Solid State*, 61(10), 2019, 1825–1830, DOI: 10.1134/S1063783419100172.
- [18] Morassi, A., Fernandez-Saez, J., Zaera, R., Loya, J.A., Resonator-based detection in nanorods, *Mechanical Systems and Signal Processing*, 93, 2017, 645–660, DOI: 10.1016/j.ymssp.2017.02.019.
- [19] Dilena, M., Dell'Oste, M. F., Fernandez-Saez, J., Morassi, A., Zaera, R., Mass detection in nanobeams from bending resonant frequency shifts, *Mechanical Systems and Signal Processing*, 116, 2019, 261–276, DOI: 10.1016/j.ymssp.2018.06.022.
- [20] Khakimov, A. G., Review of studies on the computational diagnosis of local defects of structural elements, *Multiphase Systems*, 14(1), 2019, 1–9, DOI: 10.21662/mfs2019.1.001.
- [21] He, Q., Lilley, C. M., Resonant frequency analysis of Timoshenko nanowires with surface stress for different boundary conditions, *Journal of Applied Physics*, 112, 074322, 2012, DOI: 10.1063/1.4757593.
- [22] Olsson, P. A., T., Park, H. S., Lidstrom, P. C., The influence of shearing and rotary inertia on the resonant properties of gold nanowires, *Journal of Applied Physics*, 108, 2010, 104312, DOI: 10.1063/1.3510584.
- [23] Timoshenko, S. P., Young, D. H., Weaver, W., *Vibration Problems in Engineering*, John Wiley & Sons, New York, 1974.
- [24] Rayleigh, J. W., *The Theory of Sound*, Macmillan and Company, London, 1894.
- [25] Dowell, E. A., Ilgamov, M. A., *Studies in Nonlinear Aeroelasticity*, SV. N.Y., London, Tokyo, 1988.

ORCID iD

Marat A. ILGAMOV  <https://orcid.org/0000-0002-8766-8964>

Akim G. KHAKIMOV  <https://orcid.org/0000-0003-4093-5380>



© 2021 by the authors. Licensee SCU, Ahvaz, Iran. This article is an open access article distributed under the terms and conditions of the Creative Commons Attribution-NonCommercial 4.0 International (CC BY-NC 4.0 license) (<http://creativecommons.org/licenses/by-nc/4.0/>).

How to cite this article: ILGAMOV M.A., KHAKIMOV A.G. Influence of Pressure on the Frequency Spectrum of Micro and Nanoresonators on Hinged Supports, *J. Appl. Comput. Mech.*, 7(2), 2021, 977–983. <https://doi.org/10.22055/JACM.2021.36470.2848>

